RESEARCH PAPER

PHYSICO-MECHANICAL PROPERTIES AND MICROSTRUCTURE RESPONSES OF HYBRID REINFORCED Al6063 COMPOSITES TO PKSA/SiC INCLUSION

Peter Ikubanni[1*], Makanjuola Oki[1], Adekunle Adeleke[1], Peter Omoniyi[2,3], Emmanuel Ajisegiri[1], Esther Akinlabi[2]

[1]Department of Mechanical Engineering, College of Engineering, Landmark University, Omu-Aran, Nigeria
[2]Department of Mechanical Engineering Science, University of Johannesburg, Johannesburg, South Africa
[3]Department of Mechanical Engineering, University of Ilorin, Ilorin, Nigeria

*Corresponding author: ikubanni.peter@lmu.edu.ng, tel.: +234-706-599-3936, Department of Mechanical Engineering, Landmark University, 251101, Omu-Aran, Kwara State.

ABSTRACT

The study examined the microstructure and mechanical properties of Al-Mg-Si alloy reinforced with palm kernel shell ash (PKSA) and silicon carbide (SiC). The alloy matrix was reinforced with SiC (2 - 8 wt.%) and PKSA (2 wt.%). The double stir-casting method was used to prepare the hybrid composite. The density, porosity, hardness, tensile, and fracture toughness properties of the produced samples were evaluated based on ASTM standards. Identification of phases present in the composite was done using a PANalytical Empyrean diffractometer, while the microstructural characterization was examined using a scanning electron machine with electron dispersive spectrometer attachment. The density values increase as the SiC contents in the composites increase, while the porosity percentage of all the composites were below 4%. As the reinforcement particulates increase, the mechanical properties of the reinforced composite improved with hardness value (73 – 85.5 BHN); yield strength (81 – 102 MPa); and ultimate tensile strength (123 – 133 MPa) compared with the matrix alloy of 73 BHN, 79 MPa, and 116 MPa, respectively. However, the percentage elongation and the fracture toughness of the reinforced samples reduced to 34.2 and 40.11%, respectively. The phases identified in the composites were Al, SiO_2, Fe_3Si, MgO, and SiC, which are hard but brittle strengtheners to improve the mechanical properties of the composites. The microstructure of the reinforced samples showed uniformly dispersed reinforcement in the matrix through grain refinement as assisted by the stir casting method utilized. SiC was a better strengthener as the quantity increased in the matrix compared to PKSA in the reinforced sample. The synthesized hybrid composites would be applicable as building materials such as aluminium frames and roofing sheets.

Keywords: Aluminium composite; mechanical properties; palm kernel shell ash; SiC; physical properties

INTRODUCTION

The synthesis of new engineering materials due to rising demands for high strength to weight ratio improved service performance, and cost-effective purposes are on the increase. These new engineering materials are referred to as composite materials. Composite material is a combination of two or more different chemical constituents or materials having different interphases, which separates the constituent to obtain materials with improved properties [1,2]. The motivation for synthesizing composite is the possibility of utilizing particular properties of the constituent materials in meeting specified demands [3]. One of these new engineering materials is metal matrix composites (MMCs) in which Al, Mg, Ti, Cu, and so on, are used as the matrix materials. The most preferred base alloy is aluminium because it has light-weight, has good thermal and electrical conductivity, and has high corrosion resistance [4,5].

Compared to unreinforced alloy, MMCs have superior material properties of high strength, low density, high modulus of elasticity, improved wear resistance, high specific stiffness, low thermal expansion, better thermal conductivity, and others [3,4,6,7]. In the synthesis of MMCs, ceramic/synthetic reinforcements such as SiC, TiC, B_4C, Al_2O_3, and so on, and industrial/agro-wastes using different production routes are used [1,8,9]. The use of ceramic/synthetic reinforcements in the production of MMCs at the different matrix reinforcement ratios has become a centre of attraction for researchers. Sometimes, two ceramic reinforcements are combined with aluminium alloy to produce MMCs [5,9 - 14]. Recently, the combination of ceramic and industrial/agro wastes have been utilized for the development of MMCs. This is due to the abundance of agro wastes which has been reported to pollute the environment [15 - 22].

Several studies have been done on the usage of monolithic reinforcements particulates made from agro wastes and a hybrid reinforcement of agro-waste and synthetic particulates in the production of aluminium matrix composites (AMCs). Prasad & Krishna [3] utilized rice husk ash (RHA) as a reinforcing material using aluminium A356.2 alloy as the matrix. The MMC was produced using a stir casting route in which the matrix was reinforced with 4, 6, and 8% RHA. The wear characteristics of the synthesized MMCs were investigated. The study revealed that reinforced alloy has higher hardness and wear resistance than unreinforced alloy. Hence, the RHA improved the hardness and

wear properties of the alloy. Three reinforcements (SiC, Al₂O₃, and fly ash) were employed in the production of hybrid MMCs by Gireesh et al. [23] The fly ash was made to be constant (5%) for each composition while SiC and Al₂O₃ were varied in the synthesis through stir casting route. The study reported improved hardness, high yield strength, and low rate of wear at 20 total reinforcement addition. However, there was no significant change in the value of the impact strength.

Fatile et al. [21] examined the mechanical and microstructural behaviour of AMCs produced using hybrid reinforcement of Sic and corn cob ash (CCA) via the two-step stir casting method. The study reported uniformly distributed reinforcement particulates in the Al matrix with the decrease in density, hardness, yield strength (YS), ultimate tensile strength (UTS), and specific strength as the CCA particulates increase in the composites. Investigation on the mechanical properties of RHA-SiC reinforced aluminium was also conducted by Prasad et al. [22]. The study reported a decrease in density and elongation, and an increase in hardness, porosity, YS, and UTS as the reinforcement particulates increase. However, the separate effects of each reinforcement addition were not reported in the study. The first aspect of this study characterized the composites with a constant weight percentage of SiC while the weight percentage of the PKSA varied in increasing step of 2 wt.%. It was discovered that the more the PKSA in the hybrid reinforcement, the better is the hardness and strength of the composites. However, the fracture toughness declined with increased PKSA particulates [24].

In this study, the effect of using constant weight percentage of PKSA and varied SiC particulates percentage weight in increasing step of 2wt.% in the synthesis of Al6063/2%PKSA/SiC was investigated. Therefore, the study examines the microstructural and physico-mechanical properties of the produced AMCs. ASTM standard procedures were followed in testing for the mechanical properties and scanning electron microscopy coupled with energy dispersion x-ray (SEM-EDX) was used for the internal morphology examination while X-ray diffraction was used in obtaining the phases of the AMCs developed.

MATERIAL AND METHODS

The reinforcements utilized in this study were PKSA and SiC while the matrix material was Al6063 alloy. The PKSA was obtained as presented in earlier studies [25,26]. The chemical constituents of the PKSA and Al6063 matrix alloy are displayed in **Table 1**. The SiC was obtained from a vendor in Akure, Ondo State. The composite production was through the double stir casting liquid metallurgy route. The reinforcing materials were initially pre-treated by heating to 250ºC for inorganic matter and carbonaceous material removal [27]. These were later incorporated into the molten matrix. The comprehensive technique reported for developing hybrid composite was used to produce the samples [19,26]. The nomenclature for each sample with the weight proportions of the SiC and PKSA particulates and the matrix alloy is shown in **Table 2**. **Figure 1** shows the illustrative procedures utilized in this study.

Table 1 Chemical composition (%) of the PKSA and Al6063 matrix

| PKSA										
Constituents	Na₂O	MgO	Al₂O₃	SiO₂	P₂O₅	K₂O	CaO	TiO₂	Fe₂O₃	MnO	LOI
%	0.17	3.14	6.46	66.90	3.78	5.20	5.52	0.53	5.72	0.08	2.50
Al6063 matrix										
Constituents	Si	Fe	Mn	Mg	Cu	Ti	Zn	Cr	Sn	Al	
%	0.43	0.17	0.04	0.48	0.01	0.02	0.01	0.01	0.01	Bal.	

*LOI- Loss on ignition

Table 2 Designation of composite samples produced

Sample Nomenclature	Composite mixture
AA	Pure Al 6063 alloy
AB	Al 6063 alloy/ 2% SiC
AC	Al 6063 alloy/ 2% PKSA
AD	Al 6063 alloy/ 2% PKSA/ 4% SiC
AE	Al 6063 alloy/ 2% PKSA/ 6% SiC
AF	Al 6063 alloy/ 2 % PKSA/ 8% SiC

The phases present in the produced samples were obtained using an X-ray diffractometer (XRD) (PANalytical Empyrean diffractometer), while the morphological examination of the produced composites was done with a scanning electron microscope (SEM) (Model: Vega 3 TESCAN) coupled with an electron dispersive spectrometer (EDS). The theoretical density (ρ_{th}) and experimental density (ρ_{ex}) were obtained and the values were used to determine the porosity. The theoretical density was calculated by applying the rule of mixtures, while Archimedes' principle was employed to obtain the experimental density of the composite samples [22]. The porosity was then estimated using Eq. (1).

$$Porosity = \frac{\rho_{th} - \rho_{ex}}{\rho_{th}} \qquad (1.)$$
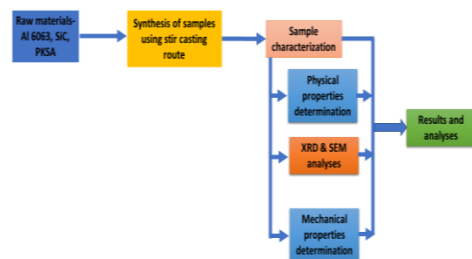
**Fig. 1** Illustration of the experimental procedure

The hardness values of the composites were obtained from a Brinell hardness testing machine in consonance with the ASTM E10-18 (2018) standard [28]. Four different indents were made on each of the samples and readings were obtained accordingly. The tensile test and fracture toughness were performed using Instron 3369 model universal testing machine following the ASTME8/E8M-16ae1 (2016) standard [29] procedures. Triplicate tests were carried out on each sample composition for the reliability of the results. Other procedures to obtain the fracture toughness values were adopted from the study of Alaneme et al. [30] For the reproducibility and repeatability of the data ob-

tained, the test was done in triplicates. Thereafter, the microstructural examination of the fractured surface of the sample was carried out with the aid of SEM/EDS equipment.

RESULTS AND DISCUSSION

Figure 2 (a) and **(b)** illustrate the XRD spectrum of the unreinforced alloy and the hybrid reinforced composites, respectively. Fig. 2(a) reveals the presence of the Al matrix as the major phase present in the unreinforced alloy. Some of the peaks or phases detected in the reinforced composites are aluminium, suessite (Fe_3Si), periclase (MgO), silica (SiO_2), and silicon carbide (SiC). Suessite is an intermetallic cubic crystal system that could be formed from the presence of ferric oxide, SiC or silica in the

hybrid reinforcement contents used. In line with the characterized PKSA in the study of Ikubanni et al. [25], these oxides are identified as hard but brittle particulates required for strengthening composite metal materials. The Al_4C_3 phase was not detected in the composite developed in this study owing to the calcination of PKS, which reduced carbon presence as well as the presence of SiO_2 in the PKSA. Bodunrin et al. [31] reported the detrimental outcome of the Al_4C_3 phase on the mechanical and corrosion behaviours of MMCs. When nanoparticles of PKSA was used as reinforcement in the Al6063 matrix, the formation of this detrimental phase was not detected [17]. Although, Mg_2SiO_4 formation was not detected in this present study silica and MgO interaction could result in its formation considering the study of Aigbodion & Ezema [17].
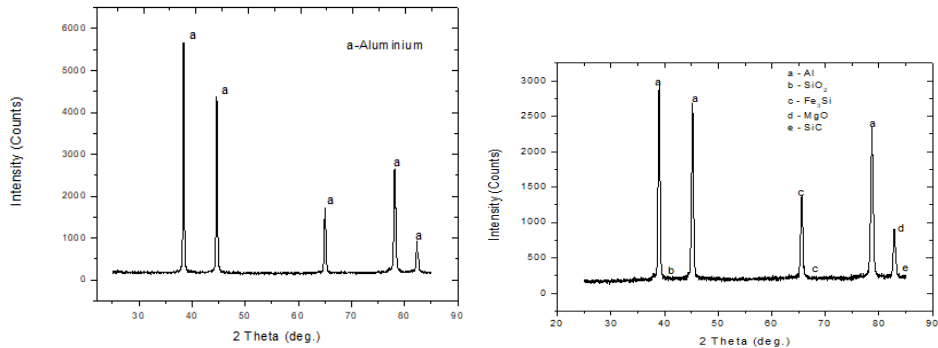
Fig. 2 (a) Unreinforced Aluminium phase (b): Hybrid reinforced aluminium composite phases

The SEM of the unreinforced alloy (AA) shown in **Fig. 3a** discloses structures without voids. The micrographs of the monolithic reinforced and hybrid reinforced composites are displayed in **Fig. 4(a)** and **Fig. 5(a)**, respectively. These micrographs show uniform and homogeneous distribution of the SiC and PKSA in the base alloy. The synthesized composites show no sign of formation of crack as well as pore enlargement as a result of the suitable process parameters employed for the composites synthesized. This suggests that an enhanced wetting ability exists between the matrix and reinforcements [16]. Due to the minimal presence of the PKSA in sample AF, the micrograph in **Fig. 5(a)**

shows more SiC particulates. The adopted synthesis process for composite in this study gave no avenue for crack formation. This is in agreement with the findings of Aigbodion[16] and Kanth et al. [18]. The low porosity of the produced composites is an indication of well-distributed reinforcement particulates as displayed in the SEM micrographs in **Figs. 4(a)** and **5(a)**. The adopted double stir-casting route used tends surface tension discontinuity between the base alloy and the reinforcing materials during stirring. This liquid metallurgical route employed is said to be reliable as air bubbles entrapped in the composite molten metal are allowed to escape during composite production [32].
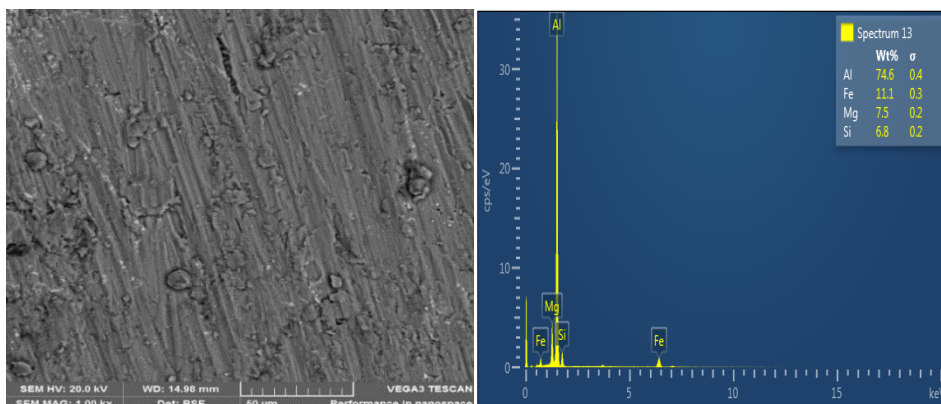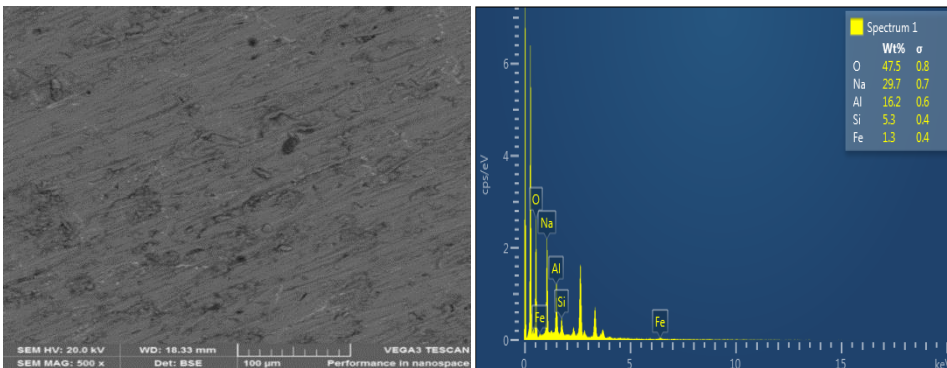

Fig. 3 (a) Micrograph (b) Elemental spectra of the unreinforced composite

Figure 3(b) is the EDS spectra for the unreinforced alloy (Sample AA). It reveals different peaks such as aluminium (Al), magnesium (Mg), silicon (Si), and iron (Fe). This confirms the basic elements present in Al 6063 (**Table 1**). **Figures 4(b)** and **5(b)** reveal the peaks of the elements obtained in **Fig. 3(b)** with the addition of some other elements like sodium (Na) and oxygen (O). From these additional elements, there is the tendency for the formation of various strengthening oxides such as alumina (Al_2O_3), silica (SiO_2), magnesium oxide (MgO), iron (III) oxide (Fe_2O_3), and oxide from sodium (Na_2O). The presence of oxygen could be derived from the PKSA constituent present in the composite as seen in **Figs. 4(b)** and **5(b)**. The EDS spectra of sample AA shows the absence of oxygen peaks.
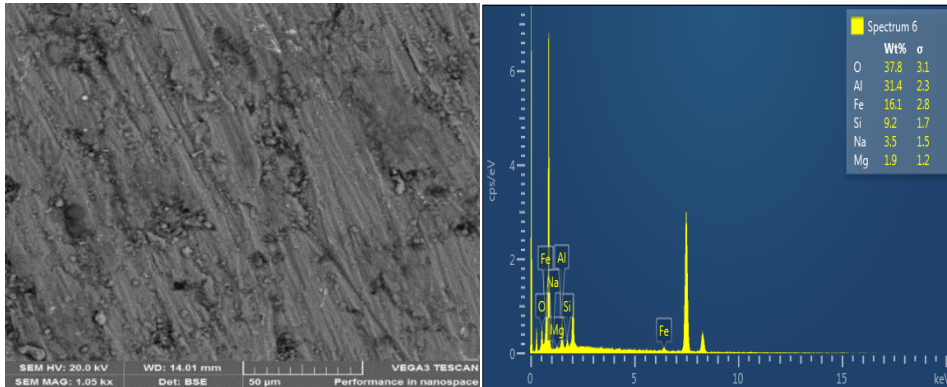
Fig. 4 (a) Micrograph (b) Elemental spectra of Sample AC

Fig. 5 (a) Micrograph (b) Elemental spectra of Sample AF

Density and porosity

Table 3 displays the outcomes of the experimental and theoretical densities of Al6063 alloy with varying reinforcement contents. Both densities of the reinforced alloy were observed to reduce slightly compared to the unreinforced alloy. However, it was observed that the density of sample AB increased slightly for the theoretical and experimental densities because of the hard nature and higher density of SiC over aluminium. The lowest value for the theoretical and experimental densities was observed to be for sample AC, were 2 wt.% PKSA and no SiC particulates were used as the reinforcement. The reduction in the densities could be attributed to the low density of PKSA particles. This is consistent with the findings of Edoziuno et al. [20], where PKS particle was said to be less dense compared to aluminium alloy. However, the gradual increment in the densities for samples AD – AF could be attributed to the gradual increment in the SiC particulate of the reinforcement while 2 wt.% PKSA was made constant for all the samples. As earlier stated, the density of SiC particulates brought slight improvement to the density of the AMCs synthesized. The utilization of SiC and bamboo leaf ash (BLA) as reinforcement in Al-Mg-Si alloy in the study of Alaneme et al. [33] showed increased density when SiC content increased, while BLA content reduced. The percentage porosity was observed to be less than 2.2%. The increased presence of SiC, a ceramic material of high density; enhanced the density of the composites. Hence, the lightweight composites achieved showed that they could be suitable for automotive applications such as in hoods, doors, and car bodies.

The difference between densities of the composites was used in the evaluation of the porosity. Porosity is a representation of the void volume to total volume fraction From **Table 3**, it was observed that the percentage porosity of the samples did not follow any increasing or decreasing pattern. However, the porosity was below 2.2%. The level of porosity could be caused by unescaped air as well as the reinforcement poor wettability [15,20]. Pores, especially when large, could serve as potential location for fracture initiation [34]. Bidulska et al. [35] stated that strain-induced porosity may have the ability to limit the material properties enhancement. The presence of magnesium in the magnesium oxide of the PKSA constituent would have enhanced the wettability of the composites synthesized. Generally, the AMCs produced

have percentage porosities that were below the optimally acceptable limit of 4% for cast MMCs [20,36]. Thus, the application of the stir-casting technique in the synthesis of MMCs is found to be very useful in producing different new products for engineering applications.

Table 3 Experimental density, theoretical density and percentage porosity

| Sample	Theoretical density (g/cm³)	Experimental density (g/cm³)	%Porosity
AA	2.700	2.6443	2.063
AB	2.710	2.6510	2.177
AC	2.660	2.6034	2.128
AD	2.680	2.6262	2.007
AE	2.690	2.6351	2.041
AF	2.700	2.6440	2.074

Mechanical properties

The hardness values of the synthesized AMCs are shown in **Fig. 7**. It was observed from **Fig. 6** that all the reinforced alloys have improved hardness values compared to the unreinforced alloy. The values of the hardness for all the produced AMCs ranged from 73 to 85.5 BHN. The sample AC showed a slight improvement in hardness value (74.09 BHN) over the un-reinforced alloy (sample AA) with a hardness value of 73.02 BHN. The slight increase of 1.44% could be accrued to the presence of dominant refractory oxides phases such as SiO_2, Al_2O_3, Fe_2O_3, and MgO in the PKSA particulates (Table 1). The refractory oxides present are chemically and naturally hard. These were also revealed in the micrographs of the synthesized composites. This is consistent with other studies [16,25]. Higher hardness of sample AB over sample AC could be linked to the higher hardness and strength of SiC particulates. It is important to re-state that sample AB has purely 2 wt.% SiC only as reinforcement, while sample AC has purely 2 wt.% PKSA only as reinforcement. However, due to the hard nature of SiC, the hardness values of samples AD – AF increased as the SiC particulate percentage weight increased with a constant of 2 wt.% PKSA. A similar observation of improvement in hardness was obtained in the study of Alaneme et al. [19], where 6 and 10 wt.% of hybrid reinforcements of SiC and groundnut shell ash (GSA) were incorporated into Al-Mg-Si alloy, respectively. As the SiC contents increase in both 6 and 10 wt.% with GSA content reduction, the hardness of the composite increases. This increase could be attributed to the abundant presence of the hard ceramic material (SiC) over the dominant refractory oxides existing in the 2 wt.% PKSA. It affirmed that reinforcement inclusion in the base alloy improved the hardness value and the reason for the improvement is the higher percentage of SiC content [10].
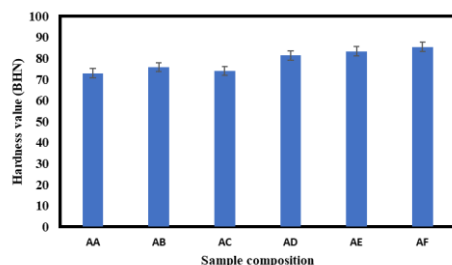
The yield strength (YS), ultimate tensile strength (UTS), and percentage elongation of the synthesized AMCs are presented in **Fig. 7**. The YS and UTS increased as the percentage weight of SiC increased in the reinforcement. When pure 2 wt.% PKSA was used as the reinforcement (Sample AC), the YS and UTS values improved compared to sample AA (un-reinforced alloy) while it declined compared to sample AB (with purely 2 wt.% SiC). The strength improvement of sample AC over sample AA could be linked to the presence of hardeners and strengtheners in the PKSA particulates. The presence of some refractory oxides in the PKSA with low hardness value and elastic modulus compared to SiC (sample AB) could be responsible for the decline in the strength of the composites (Sample AC). This is because the presence of PKSA reduced the reinforcing phase's load-bearing capacity. However, because the strength of PKSA is lower than SiC, the YS and UTS values dropped compared to sample AB. The further rise in YS and UTS for other samples (Samples AD – AF) was due to the hard nature of SiC increment in the composites. This observation is consistent with several other studies [10, 18, 37, 38]. The rise in YS and UTS with the samples with SiC could indicate higher bonding strength between the SiC particulates and the matrix alloy during the continual stirring production process, which could cause grain enhancement for even reinforcement distribution in the alloy [15, 37, 3]. In metallic materials, several factors significantly impact their mechanical properties. These factors include, but are not limited to; grain boundaries, second phases, sub-structures, and solid solutions [39]. The revelation of grain refinement of the matrix alloy and the reinforcing particulates through the micrographs of the produced composites showed it was the major influencer of the tensile strength. The reinforcement particulates play a germane role in the load transfer in giving strength to the synthesized composites. Grain boundaries are obtained through matrix-reinforcing particles atom bonding interface. Furthermore, the reinforcements and matrix have different coefficients of thermal expansion, which could lead to thermal mismatch in the interface during the composite solidification process. As a result, the matrix interface could yield into plastic deformation [31]. This could produce higher yield and tensile strength values. The percentage elongation indicates the ductility of the synthesized composite and it exhibited a declining trend as the particulate reinforcements were increasingly introduced into the alloy as shown in **Fig. 8**. The un-reinforced alloy showed better ductility than the reinforced alloys. The ductility of sample AC (7.4%) was better than that of sample AB (7.2%). This is because the relative hardness of PKSA particulates was lower than that of SiC particulates. However, when the SiC particulates in the composites increased, there was a noticeable drop in the ductility. As reported by Yigezu et al. [37], the relative hardness of SiC particulates could be attributed to the cause of the low/declining ductility. This is because SiC particles are prone to the initiation of localized crack, which increased the brittle effect at

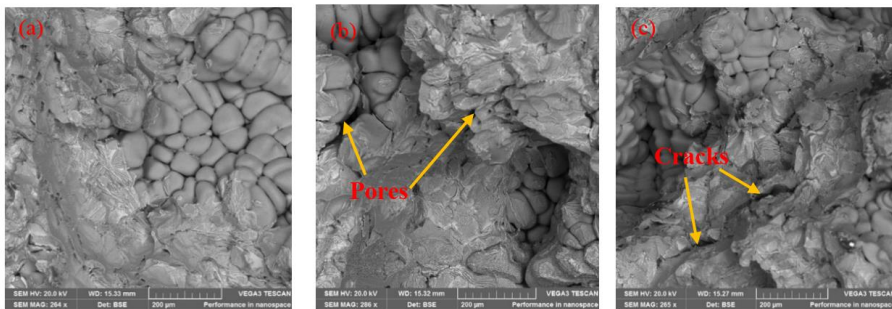**Fig. 6** Hardness values of the synthesized composite samples
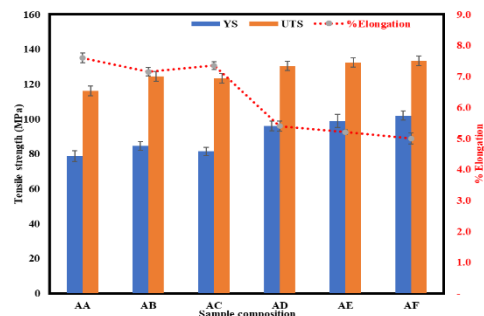
Fig. 7 Strengths and strain to fracture of the synthesized samples

the reinforcement-matrix boundary as a result of localized stress concentration spots [37, 40]. The developed composites in this study when subjected to high straining will fail quickly. Hence, the composites will find applications in producing window and door frames in buildings as well as in areas that require less ductility.

Figure 8 showed the fracture toughness of the samples composite synthesized. Sample AA has the highest value of fracture toughness of 12.49 MPa m$^{1/2}$. The fracture toughness value of Sample AB was reduced to 10.14 MPa m$^{1/2}$ because of the presence of hard SiC particulates. However, the addition of monolithic reinforcement of PKSA (2 wt.%) in sample AC gave a better fracture toughness value compared to sample AB, with a 4.2 % improvement. The decreasing values of the fracture toughness of samples AD – AF could be attributed to the incremental presence of SiC particulate in the hybrid reinforcement. SiC has been reported to have a greater propensity to undergo crack propagation rapidly. The same observation was reported by Milan & Bowen [41]. Fracture toughness of composite materials can be influenced through the introduction of reinforcements into metal matrix that would minimize interparticle arrangement as well as generate strong obstacle to open the crack front [42,43]. With regards to the particulate volume fraction effects of the SiC on the MMCs, the more the particulate volume, the smaller the interparticle spacings with a larger amount of clustering sites. This is the reason for higher tensile strength with reduced ductility and fracture toughness of MMCs [41]. More so, the primary fracture mechanisms have been linked to being facilitated by the individual or combination of particle cracking, interfacial cracking, or particle debonding [19,44].
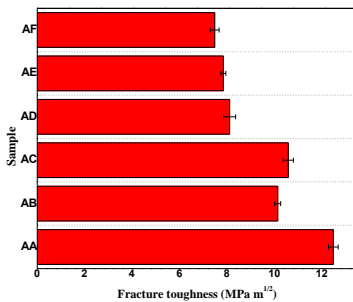
Fig. 8 Fracture toughness of the synthesized samples

Microstructural examination of the fractured surface

Basically, fracture occurrence in composite materials is through initiation of crack which proceeds at the debonded interface between the matrix and the reinforcement [45]. **Figure 9 (a) – (c)** display the fractured surface morphologies of the composite samples. The SEM image of the unreinforced matrix is shown in **Fig. 9 (a)**. The micrograph revealed cup and cap surfaces as well as some populations of dimples. Dimples are associated with ductility, that is; a finer dimple size relates to higher ductility and vice-versa [46]. The unreinforced matrix showed better ductility before eventual necking and breaking. This is due to the non-involvement of the reinforcement. **Figures 9 (b) and (c)** display the fractured surface micrographs. The fractured surfaces also showed cup and cap surfaces. The large pores were seen in **Fig. 9(b)** owing to the usage of weak PKSA as the only reinforcement in the matrix alloy. A high presence of well-developed dimples was revealed from the fractured surface of the unreinforced Al matrix. There is a minimal necking formation before the composites eventually fractured. The fractured surface of the composites displayed a mixed fracture mechanism due to the ductility of the alloy as well as the brittle fracture of the reinforcing particulates. The composites failure could also be assigned to the detrimental weak PKSA phases through the formation of intermetallic phases that activates the fracture mode

The physical, mechanical and microstructural properties of hybrid reinforced (PKSA and SiC) aluminium matrix composites were studied. The double stir casting used for the production of the composites was found reliable as porosity was found to be lower than 2.5% due to the homogeneous distribution of the reinforcements. The composites revealed the presence of some compounds and intermetallic, which include SiO_2, MgO, SiC, and intermetallic (Fe_3Si) obtained from the phase analyses. Their presence helps to enhance the strength and hardness of the composites. The density of the composites increased as the SiC contents increased. The density of the composites reinforced with 2%PKSA was lower than that reinforced with 2% SiC. The SiC increment with constant 2% PKSA particulates in the matrix enhanced the hardness value, yield strength, ultimate tensile strength, while the percentage elongation and fracture toughness of the synthesized composites were reduced. A mixed fracture mechanism was noticed owing to the SiC presence, which results in composite failure via rapid crack propagation. The composites developed is recommended for use in light-weight engineering applications.

Fig. 9 SEM fractured surface of (a) unreinforced alloy (b) 2% PKSA reinforced composite (c) hybrid reinforcement (2% PKSA-8% SiC) composite

CONCLUSION

The physical, mechanical and microstructural properties of hybrid reinforced (PKSA and SiC) aluminium matrix composites

were studied. The double stir casting used for the production of the composites was found reliable as porosity was found to be lower than 2.5% due to the homogeneous distribution of the reinforcements. The composites revealed the presence of some

compounds and intermetallic, which include SiO_2, MgO, SiC, and intermetallic (Fe_3Si) obtained from the phase analyses. Their presence helps to enhance the strength and hardness of the composites. The density of the composites increased as the SiC contents increased. The density of the composites reinforced with 2%PKSA was lower than that reinforced with 2% SiC. The SiC increment with constant 2% PKSA particulates in the matrix enhanced the hardness value, yield strength, ultimate tensile strength, while the percentage elongation and fracture toughness of the synthesized composites were reduced. A mixed fracture mechanism was noticed owing to the SiC presence, which results in composite failure via rapid crack propagation. The composites developed is recommended for use in light-weight engineering applications.

REFERENCES
1. P.P. Ikubanni, M. Oki, A.A. Adeleke: Cogent Engineering, 7, 2020, 1–19. https://doi.org/10.1080/23311916.2020.1727167.
2. T.A. Orhadahwe, O.O. Ajide, A.A. Adeleke, P.P. Ikubanni: Arab Journal of Basic and Applied Science. 27, 2020. https://doi.org/10.1080/25765299.2020.1830529.
3. D.S Prasad, A. Rama Krishna:. Journal of Material Science and Technology. 28, 2012, 367–372. https://doi.org/10.1016/S1005-0302(12)60069-3.
4. K. Halil, O. Ismail, D. Sibel, Ç. Ramazan: Journal of Material Research and Technology, 8, 2019, 5348–5361. https://doi.org/10.1016/j.jmrt.2019.09.002.
5. H.C. Ananda Murthy, S.K. Singh: Advanced Materials Letters, 6, 2015, 633–640. https://doi.org/10.5185/amlett.2015.5654.
6. K.K. Alaneme, K.O. Aluko: Scientica Iranica A, 19, 2012, 992–996. https://doi.org/10.1016/j.scient.2012.06.001.
7. P. Ravindran, K. Manisekar, S. Vinoth Kumar, P. Rathika: Materials and Design, 51, 2013, 448-456. https://dx.doi.org/10.1016/j.matdes.2013.04.015.
8. M.G.A. Prasad, N. Bandekar: Journal of Material Science and Chemical Engineering, 3, 2015, 1–8. https://doi.org/10.4236/msce.2015.33001.
9. S. Arivukkarasan, V. Dhanalakshmi, B. Stalin, M. Ravichandran: Particulate Science and Technology, 36, 2018, 967–973. https://doi.org/10.1080/02726351.2017.1331285.
10. P.V. Reddy, P.R. Prasad, D.M. Krishnudu, E.V. Goud: Journal of Bio- and Tribo-Corrosion, 5, 2019, 1–10. https://doi.org/10.1007/s40735-019-0282-0.
11. M.B.A. Shuvho, M.A. Chowdhury, M. Kchaou, B.K. Roy, A. Rahman, M.A. Islam: Chemical Data Collection, 28, 2020. https://doi.org/10.1016/j.cdsc.2020.100442.
12. M. Nagaral, V. Auradi, S.A. Kori, V. Hiremath: Journal of Mechanical Engineering and Sciences, 13, 2019, 4623–4635. https://doi.org/10.15282/jmes.13.1.2019.19.0389.
13. G. Singh, S. Goyal S: Particulate Science and Technology, 36, 2018, 154–161. https://doi.org/10.1080/02726351.2016.1227410.
14. A.J. Knowles, X. Jiang, M. Galano, F. Audebert: Journal of Alloys and Compounds, 615, 2014, S401-S405. http://doi.org/10.1016/j.jallcom.2014.01.134.
15. K.K. Alaneme, M.H. Adegun, A.G. Archibong, E.A. Okotete: Journal of Chemical Technology and Metallurgy, 54, 2019, 1361–1370.
16. V.S. Aigbodion: Journal of Material Research and Technology, 8, 2019, 6011–6020. https://doi.org/10.1016/j.jmrt.2019.09.075.
17. V.S. Aigbodion, I.C. Ezema: Defence Technology, 16,

2020, 731–736. https://doi.org/10.1016/j.dt.2019.05.017.
18. U.R. Kanth, P. Rao, M..G. Krishna: Journal of Material Research and Technology, 8, 2019, 737–744. https://doi.org/10.1016/j.jmrt.2018.06.003.
19. K.K. Alaneme, M.O. Bodunrin, A.A. Awe: Journal of King Saud University- Engineering Sciences, 30, 2018, 96–103. https://dx.doi.org/10.1016/j.jksues.2016.01.001.
20. F.O. Edoziuno, A.A. Adediran, B.U. Odoni, O.G. Utu, A. Olayanju: Materials Today: Proceedings, 38, 2021, 652–657. https://doi.org/10.1016/j.matpr.2020.03.641.
21. O.B. Fatile, J.I. Akinruli, A.A. Amori: International Journal of Enngineering and Technology Innovation, 4, 2014, 251–259.
22. D.V. Prasad, C. Shoba, N, Ramanaiah: Journal of Materials Research and Technology, 3, 2014, 79–85. https://doi.org/10.1016/j.jmrt.2013.11.002.
23. C.H. Gireesh, K. Durga Prasad, K. Ramji: Journal of Composite Science, 49, 2018, 1–10. https://doi.org/10.3390/jcs2030049.
24. P.P. Ikubanni, M. Oki, A.A. Adeleke, P.O. Omoniyi: Scientific Reports, 11, 2021(14845). https://doi.org/10.1038/s41598-021-94420-0.
25. P.P. Ikubanni, M. Oki, A.A. Adeleke, A.A. Adediran, O.S. Adesina: Results in Engineering, 8, 2020, 1-9. https://doi.org/10.1016/j.rineng.2020.100173.
26. P.P. Ikubanni, M. Oki, A.A. Adeleke, A.A. Adediran, O.O. Agboola, O. Babayeju, N. Egbo, I.M.B. Omiogbemi: Material Today Proceedings, 2021. https://doi.org/10.1016/j.matpr.2021.03.537.
27. D. Siva, C. Shoba: Experimental evaluation onto the damping behavior of Al/SiC/RHA hybrid composites. Journal of Materials Research and Technology, 5, 2016, 123–130. http://dx.doi.org/10.1016/j.jmrt.2015.08.001.
28. ASTM E10-18, Standard Test Methods for Brinell Hardness of Metallic Materials, ASTM International, West Conshohocken, PA, 2018. www.astm.org.
29. ASTME8/E8M-16ae1, Standard Test Methods for Tension Testing of Metallic Materials, ASTM International, West Conshohocken, PA, 2016. www.astm.org.
30. K.K. Alaneme, C.A. Oganbule, A.A Adewale: Journal of Chemical Technology and Metallurgy, 55, 2020, 469–478.
31. M.O. Bodunrin, K.K. Alaneme, L.H. Chown: Journal of Materials Research and Technology, 4, 2015, 434–445. https://doi.org/10.1016/j.jmrt.2015.05.003.
32. K.K. Alaneme, A.V. Fajemisin, N.B. Maledi: Journal of Materials Research and Technology, 8, 2019, 670–682. https://doi.org/10.1016/j.jmrt.2018.04.019.
33. K.K. Alaneme, B.O. Ademilua, M.O. Bodunrin: Tribology in Industry, 35, 2013, 25–35.
34. P. Beiss, M. Dalgic: Materials Chemistry and Physics, 67, 2001, 37–42. https://doi.org/10.1016/S0254-0584(00)00417-X.
35. J. Bidulská, R. Bidulský, M. A. Grande, T. Kvackaj: Materials, 12, 2019, 3724. https://doi.org/10.3390/ma12223724.
36. K.K. Alaneme, O.K. Sanusi: Engineering Science and Technology- an International Journal, 18, 2015, 416–422. https://doi.org/10.1016/j.jestch.2015.02.003.
37. B.S. Yigezu, M.M. Mahapatra, P.K. Jha: Journal of Minerals and Materials Characterization and Engineering, 1, 2013, 124–130. https://dx.doi.org/10.4236/jmmce.2013.14022.
38. G.B.V. Kumar, P. Prasad, N. Suresh, R. Pramod, C.S.P. Rao: Composites Part B, 175, 2019, 1-11. http://dx.doi.org/10.1016/j.compositesb.2019.107138.
39. C.U. Atuanya, A.O.A. Ibhadode, I.M. Dagwa: Results in Physics, 2, 2012, 142–149. http://dx.doi.org/10.1016/j.rinp.2012.09.003.
40. K.K. Alaneme, M.O. Bodunrin: Mechanical behaviour of alumina reinforced AA 6063 metal matrix composites developed by two-stir casting process. Acta Technic Corvininesis-Bulletin of Engineering, 6, 2013, 105–110.

41. M.T. Milan, P. Bowen: Journal of Materials Engineering and Performance, 13, 2004, 775–783. https://doi.org/10.1361/10599490421358.

42. D.B. Niranjan, G.S. Shiva Shankar, L.B. Shankar: MATEC Web of Conferences 144, 2018, 02012. https://doi.org/10.1051/matecconf/201814402012.

43. H. Guddhur, C. Naganna, S. Doddamani: An International Journal of Optimization and Control: Theories & Applications, 11, 2021, 152 – 157. https://doi.org/10.11121/ijocta.01.2021.00990.

44. K.K. Alaneme, T.M. Adewale: Tribology in Industry, 35, 2013, 163–172.

45. A.M. Maleque, A.A. Adebisi, N. Izzati: IOP Conference Series: Materials Science and Engineering, 184, 2017, 012031. https://doi.org/10.1088/1757-899X/184/1/012031.

46. M.C. Gowri Shankar, S.S. Sharma, U.K. Achutha, H.G. Pavan: Journal of Materials and Environmental Sciences, 8, 2017, 257 – 263.